

# HEALPix — a Framework for High Resolution Discretization, and Fast Analysis of Data Distributed on the Sphere

K. M. Górski<sup>1,2</sup>, E. Hivon<sup>3,4</sup>, A. J. Banday<sup>5</sup>, B. D. Wandelt<sup>6,7</sup>, F. K. Hansen<sup>8</sup>, M. Reinecke<sup>5</sup>, M. Bartelman<sup>9</sup>

<sup>1</sup> *JPL/Caltech, M/S 169/327, 4800 Oak Grove Drive, Pasadena CA 91109*

<sup>2</sup> *Warsaw University Observatory, Aleje Ujazdowskie 4, 00-478 Warszawa, Poland*

<sup>3</sup> *Observational Cosmology, MS 59-33, Caltech, Pasadena, CA 91125*

<sup>4</sup> *IPAC, MS 100-22, Caltech, Pasadena, CA 91125*

<sup>5</sup> *Max-Planck-Institut für Astrophysik, Karl-Schwarzschild-Str.*

*1, Postfach 1317,*

*D-85741 Garching bei München, Germany*

<sup>6</sup> *Department of Physics, University of Illinois, Urbana, IL 61801*

<sup>7</sup> *Department of Astronomy, UIUC, 1002 W. Green Street, Urbana, IL 61801*

<sup>8</sup> *Dipartimento di Fisica, Università di Roma 'Tor Vergata', Via della Ricerca Scientifica*

*1, I-00133 Roma, Italy*

<sup>9</sup> *ITA, Universität Heidelberg, Tiergartenstr. 15, D-69121 Heidelberg, Germany*

## ABSTRACT

HEALPix – the Hierarchical Equal Area iso-Latitude Pixelization – is a versatile data structure with an associated library of computational algorithms and visualization software that supports fast scientific applications executable directly on very large volumes of astronomical data and large area surveys in the form of discretized spherical maps. Originally developed to address the data processing and analysis needs of the present generation of cosmic microwave background (CMB) experiments (e.g. BOOMERanG, WMAP), HEALPix can be expanded to meet many of the profound challenges that will arise in confrontation with the observational output of future missions and experiments, including e.g. Planck, Herschel, SAFIR, and the Beyond Einstein CMB polarization probe. In this paper we consider the requirements and constraints to be met in order to implement a sufficient framework for the efficient discretization and fast analysis/synthesis of functions defined on the sphere, and summarise how they are satisfied by HEALPix.

*Subject headings:* cosmic microwave background — cosmology: observations — methods: statistical

## 1. Introduction

Advanced detectors in modern astronomy produce data at huge rates at many wavelengths. Some data sets are becoming very impressively large indeed. Of particular interest to us are those that accumulate astronomical data distributed on the entire sky, or a considerable fraction thereof. Typical examples include radio, cosmic microwave background, submillimeter, infrared, X-ray, and gamma-ray sky maps of diffuse emission, and full sky or wide area surveys of extragalactic objects. Together with the wealth of gathered information comes the inevitable burden of increased complexity of the tasks of data reduction and science extraction. In this paper we are focused on those issues, which are related to the distinctive nature of the spherical spatial domain over which the data reside, and need to be analysed for scientific return. Our original motivations come from work in the field of measurement and interpretation of the cosmic microwave background (CMB) anisotropy. The growing complexity of the CMB anisotropy science extraction problem can be illustrated by the transition between the data sets of COBE-DMR (early 1990s, 7 deg resolution, 6000 pixel sky maps at 3 wavelengths), Boomerang (late 1990s, FWHM 12 arcmin, partial sky maps of 200000 pixels at 4 wavelengths), WMAP (early 2000s, resolution up to FWHM 14 arcmin, 3 million pixel sky maps at 5 wavelengths), and Planck (data expected 2008, resolution up to FWHM 5 arcmin, 50 million pixel sky maps at 9 wavelengths). Science extraction from these data sets involves (1) global analysis problems – harmonic decomposition, estimation of the power spectrum and higher order measures of spatial correlations, (2) simulations of models of the primary and foreground sky signals to study instrument performance, and calibrate foreground separation and statistical inference methods, (3) real space morphological analyses, object detection, identification, and characterization, and (4) spatial and/or spectral cross-correlation with external data sets. These tasks, and many others, necessitate a careful definition of the data models, and proper set-up of the mathematical framework of data analysis such that the algorithmic and computing time requirements can be satisfied in order to achieve successful scientific interpretation of expensive and precious observations. A particular method of addressing some of these problems is described next.

## 2. Discretized Mapping and Analysis of Functions on the Sphere

The analysis of functions on domains with spherical topology occupies a central place in physical science and engineering disciplines. This is particularly apparent in the fields of astronomy, cosmology, geophysics, atomic and nuclear physics. In many cases the geometry is either dictated by the object under study or approximate spherical symmetry can be exploited to yield powerful perturbation methods. Practical limits for the purely analytical

study of these problems create an urgent necessity for efficient and accurate numerical tools.

The simplicity of the spherical form belies the intricacy of global analysis on the sphere. There is no known point set which achieves the analogue of uniform sampling in Euclidean space and allows exact and invertible discrete spherical harmonic decompositions of arbitrary but band-limited functions. Any existing proposition of practical schemes for the discrete treatment of such functions on the sphere introduces some (hopefully small) systematic error dependent on the global properties of the point set. The goal is to minimise these errors and faithfully represent deterministic functions as well as realizations of random variates both in configuration and Fourier space while maintaining computational efficiency.

We illustrate these points using as an example the field of Cosmic Microwave Background (CMB) anisotropies. Here we are already in a situation of an ongoing rapid growth of the volume of the available data. The NASA’s Wilkinson Microwave Anisotropy Probe (WMAP) already is, and ESA’s Planck will (in the near future) be aiming to provide multi-frequency, high resolution, full sky measurements of the anisotropy in both temperature and polarization of the cosmic microwave background radiation. The ultimate data products of these missions — multiple microwave sky maps, each of which will have to comprise more than  $\sim 10^6$  pixels in order to render the angular resolution of the instruments — will present serious challenges to those involved in the analysis and scientific exploitation of the results of both surveys.

A digitized sky map is an essential intermediate stage in information processing between the entry point of data acquisition by the instruments — very large time ordered data streams, and the final stage of astrophysical analysis — typically producing a ‘few’ numerical values of physical parameters of interest. *COBE*-DMR sky maps (angular resolution of  $7^\circ$  (FWHM) in three frequency bands, two channels each, 6144 pixels per map) were considered large at the time of their release. As for the presently available (WMAP) and future CMB maps, a whole sky CMB survey at the angular resolution of  $\sim 10'$  (FWHM), discretized with a few pixels per resolution element (so that the discretisation effects on the signal are sub-dominant with respect to the effects of instrument’s angular response), will require map sizes of at least  $N_{pix} \sim \text{a few} \times 1.5 \cdot 10^6$  pixels. Even more pixels than that will be needed to represent the Planck-HFI higher resolution high-frequency channels.

This estimate,  $N_{pix}$ , should be multiplied by the number of frequency bands (or, indeed, by the number of individual observing channels — 74 in the case of Planck — for the analysis work to be done before the final coadded maps are made for each frequency band) to render an approximate expected size of the already very compressed form of survey data which would be the input to the astrophysical analysis pipeline.

Hence, a careful attention ought to be given to devising high resolution CMB map

structures which can maximally facilitate the forthcoming analyses of large size data sets, especially so because many essential scientific questions can only be answered by *global* studies of such data sets.

This paper describes the essential geometric and algebraic properties of our method of digital representation of functions on the sphere — the Hierarchical Equal Area and isoLatitude Pixelization (HEALPix) — and the associated multi-purpose computer software package. We have originally devised HEALPix, and we started distributing HEALPix software to the community in 1997. Presently HEALPix software is distributed from the web-site [www.eso.org/science/healpix](http://www.eso.org/science/healpix).

### 3. Requirements for a Spherical Pixelization Scheme

Numerical analysis of functions on the sphere involves (1) a class of mathematical operations, whose objects are (2) discretised maps, i.e. quantizations of arbitrary functions according to a chosen tessellation (exhaustive partition of the sphere into finite area elements). Hereafter we mostly specialise our discussion to CMB related applications of HEALPix, but all our statements hold true generally for any relevant deterministic and random functions on the sphere.

Considering point (1): Standard operations of numerical analysis which one might wish to execute on the sphere include convolutions with local and global kernels, Fourier analysis with spherical harmonics and power spectrum estimation, wavelet decomposition, nearest-neighbour searches, topological analysis, including searches for extrema or zero-crossings, computing Minkowski functionals, extraction of patches and finite differencing for solving partial differential equations. Some of these operations become prohibitively slow if the sampling of functions on the sphere, and the related structure of the discrete data set, are not designed carefully.

Regarding point (2): Typically, a whole sky map rendered by a CMB experiment contains (i) signals coming from the sky, which are by design strongly band-width limited (in the sense of spatial Fourier decomposition) by the instrument's angular response function, and (ii) a projection into the elements of a discrete map, or pixels, of the observing instrument's noise; this pixel noise should be random, and white, at least near the discretisation scale, with a band-width significantly exceeding that of all the signals.

With these considerations in mind we proposed the following list of desiderata for the mathematical structure of discrete whole sky maps:

1. **Hierarchical structure of the database.** This is recognized as essential for very large data bases, and was indeed postulated already in construction of the Quadrilateralized Spherical Cube (or QuadCube, see White & Stemwedel (1992), and [http://lambda.gsfc.nasa.gov/product/cobe/skymap\\_info\\_new.cfm](http://lambda.gsfc.nasa.gov/product/cobe/skymap_info_new.cfm)), which was used for all the *COBE* data. A simple argument in favour of this states that the data elements which are nearby in a multi-dimensional configuration space (here, on the surface of a sphere), are also nearby in the tree structure of the data base. This property facilitates various topological methods of analysis, and allows for easy construction of wavelet transforms on triangular and quadrilateral grids through fast look-up of nearest neighbors.
2. **Equal areas of discrete elements of partition.** This is advantageous because white noise at the sampling frequency of the instrument gets integrated exactly into white noise in the pixel space, and sky signals are sampled without regional dependence (although still care must be taken to choose a pixel size sufficiently small compared to the instrumental resolution to avoid excessive, and pixel shape dependent, signal smoothing).
3. **Iso-Latitude distribution of discrete area elements on a sphere.** This property is essential for computational speed in all operations involving evaluations of spherical harmonics. Since the associated Legendre polynomials are evaluated via slow recursions, any sampling grid deviations from an iso-latitude distribution result in a prohibitive loss of computational performance with the growing number of sampling points.

Various known sampling distributions on a sphere have been used for the discretisation and analysis of functions (for example, see Driscoll & Healy (1994), Muciaccia, Natoli & Vittorio (1998) — rectangular grids, Baumgardner & Frederickson (1985), Tegmark (1996) — icosahedral grids, Saff & Kuijlaars (1997), Crittenden & Turok (1998) — 'igloo' grids, and Szalay & Brunner (1998) — a triangular grid), but each fails to meet simultaneously all of these requirements. In particular,

i) Quadrilateralized Spherical Cube obeys points 1 and (approximately) 2, but fails on point 3, and cannot be used for efficient Fourier analysis at high resolution.

ii) Equidistant Cylindrical Projection, a very common computational tool in geophysics, and climate modeling, and recently implemented for CMB work (Muciaccia, Natoli, Vittorio, 1998), satisfies points 1 and 3, but by construction fails with point 2. This is a nuisance from the point of view of application to full sky survey data due to wasteful oversampling near the poles of the map (or - while angular resolution of the measurements is fixed by the

instrument and does not vary over the sky, the map resolution, or pixel size, depends on the distance from the poles).

iii) Hexagonal sampling grids with icosahedral symmetry perform superbly in those applications where near uniformity of sampling on a sphere is essential (Saff, Kuijlaars, 1997), and can be devised to meet requirement 2 (see e.g. Tegmark 1996). However, by construction they fail *both* points 1 and 3.

iv) Igloo-type constructions are devised to satisfy point 3 (E. Wright, 1997, private communication; Crittenden & Turok, 1998). Point 2 can be satisfied to reasonable accuracy if quite a large number of base-resolution pixels is used( which, however, precludes efficient construction of simple wavelet transforms). Conversely, a tree-structure seeded with a small number of base-resolution pixels forces significant variations in both area and shape of the pixels.

v) GLESP construction (Doroshkevich et al 2003) takes advantage of the Gauss-Legendre quadrature to render high accuracy of numerical integration, but allows irregular variations in pixel area and is not hierarchical — in fact it offers no relation between the tessellations derived at different resolutions.

#### 4. Meeting the Requirements

All the requirements introduced in section 3. are satisfied by the class of spherical tessellations structured as follows.

First let us assume that the sphere is partitioned into a number of curvilinear quadrilaterals, which constitute the base level tessellation. If there exists a mapping of each element of partition onto a square  $[0, 1] \times [0, 1]$ , a nested  $n \times n$  subdivision of the square into ever diminishing sub-elements obtains trivially, and a hierarchical tree structure of resulting database follows. For example, a  $2 \times 2$  partition renders a quadrilateral tree, which admits an elegant binary indexation (illustrated in Fig. 1) previously employed in construction of the QuadCube spherical pixelization.

Next, let us consider the base level spherical tessellation. An entire class of such tessellations can be constructed as illustrated in Figs. 2, and 3. These constructions are characterized by two parameters:  $N_\theta$  - a number of the base-resolution pixel layers between the north and south poles, and  $N_\phi$  - a multiplicity of the meridional cuts, or the number of equatorial, or circum-polar base-resolutions pixels. Obviously, the total number of base-resolution pixels is equal to  $N_{pix} = N_\theta \times N_\phi$ , and the area of each one of them is equal to

$\Omega_{pix} = 4\pi/N_\theta/N_\phi$ . One may also notice (see Fig. 2) that each tessellation includes two single layers of polar cup pixels (with or without an azimuthal twist in their respective positions on the sphere for odd, and even values of  $N_\theta$ , respectively), and an  $N_\theta - 2$  layers of equatorial zone pixels, which form a regular rhomboidal grid in the cylindrical projection of the sphere. Since the cylindrical projection is an area preserving mapping, this property immediately illustrates that the areas of equatorial zone pixels are all equal, and to meet our requirement of fully equal area partition of the sphere, we need to demonstrate that our constructions render identical areas of the polar pixels as well. Indeed, this allows to formulate a constraint on the latitude  $\theta_\star$  at which the lateral vertices of both polar and equatorial pixels meet:

$$2\pi \times (1 - \cos \theta_\star) = N_\phi \times \Omega_{pix}/2, \quad \text{hence} \quad \cos \theta_\star = (N_\theta - 1)/N_\theta. \quad (1)$$

The curvilinear quadrilateral pixels of this tessellation class retain equal areas, but vary in shape depending on their positions on the sphere. We have chosen the  $N_\theta = 3$ , and  $N_\phi = 4$  grid (middle row, right column in both Figs. 2, and 3) for definition of our digital full sky map data standard, and named it the HEALPix grid (Górski et al. 1998). This grid is the basis for development of the HEALPix software, and it is described in more detail in the next section.

## 5. The HEALPix Grid

The requirements formulated in Sec.3 are satisfied by construction with the Hierarchical Equal Area, iso-Latitude Pixelisation (**HEALPix**) of the sphere, which is shown in Figure (4). This Figure demonstrates that HEALPix is built geometrically as a self-similar, refinable quadrilateral mesh on the sphere. The base-resolution comprises twelve pixels in three rings around the poles and equator. The resolution of the grid is expressed by parameter  $N_{side}$  which defines the number of divisions along the side of a base-resolution pixel that is needed to reach a desired high-resolution partition. All pixel centers are placed on rings of constant latitude, and are equidistant in azimuth (on each ring). All iso-latitude rings located between the upper and lower corners of the equatorial base-resolution pixels (i.e.  $-2/3 < \cos \theta_\star < 2/3$ ), or in the equatorial zone, are divided into the same number of pixels:  $N_{eq} = 4 \times N_{side}$ . The remaining rings are located within the polar cap regions ( $|\cos \theta_\star| > 2/3$ ) and contain a varying number of pixels, increasing from ring to ring, with increasing distance from the poles, by one pixel within each quadrant.

A HEALPix map has  $N_{pix} = 12N_{side}^2$  pixels of the same area  $\Omega_{pix} = \frac{\pi}{3N_{side}^2}$ .

### 5.1. Pixel Positions

Locations on the sphere are defined by  $(z \equiv \cos \theta, \phi)$  where  $\theta \in [0, \pi]$  is the colatitude in radians measured from the North Pole and  $\phi \in [0, 2\pi]$  is the longitude in radians measured Eastward.

For a resolution parameter  $N_{\text{side}}$ , the pixels are layed out on  $4N_{\text{side}} - 1$  iso-latitude rings, and can be ordered using the pixel index  $p \in [0, N_{\text{pix}}]$  running around those rings from the North to South pole.

Pixel centers on the northern hemisphere are given by the following equations:

North polar cap — for  $p_h = (p + 1)/2$ , the ring index  $1 \leq i < N_{\text{side}}$ , and the pixel-in-ring index  $1 \leq j \leq 4i$

$$i = I(\sqrt{p_h - \sqrt{I(p_h)}}) + 1 \quad (2)$$

$$j = p + 1 - 2i(i - 1) \quad (3)$$

$$z = 1 - \frac{i^2}{3N_{\text{side}}^2} \quad (4)$$

$$\phi = \frac{\pi}{2i} \left( j - \frac{s}{2} \right), \quad \text{and} \quad s = 1 \quad (5)$$

North equatorial belt — for  $p' = p - 2N_{\text{side}}(N_{\text{side}} - 1)$ ,  $N_{\text{side}} \leq i \leq 2N_{\text{side}}$ , and  $1 \leq j \leq 4N_{\text{side}}$

$$i = I(p'/4N_{\text{side}}) + N_{\text{side}} \quad (6)$$

$$j = (p' \bmod 4N_{\text{side}}) + 1 \quad (7)$$

$$z = \frac{4}{3} - \frac{2i}{3N_{\text{side}}} \quad (8)$$

$$\phi = \frac{\pi}{2N_{\text{side}}} \left( j - \frac{s}{2} \right), \quad \text{and} \quad s = (i - N_{\text{side}} + 1) \bmod 2, \quad (9)$$

where the auxilliary index  $s$  describes the phase shifts along the rings, and  $I(x)$  is the largest integer number smaller than  $x$ .

Pixel center positions on the Southern hemisphere are obtained by the mirror symmetry of the grid with respect to the Equator ( $z = 0$ ).

Defining  $\Delta z$  and  $\Delta \phi$  as the variation of  $z$  and  $\phi$  when  $i$  and  $j$  are respectively increased by unity, one can check that discretized area element  $|\Delta z \Delta \phi| = \Omega_{\text{pix}}$ , i.e. it is a constant.



## 5.2. Pixel Indexing

Specific geometrical properties allow HEALPix to support two different numbering schemes for the pixels, as illustrated in the Figure (5).

First, one can simply count the pixels moving down from the north to the south pole along each iso-latitude ring. It is in this scheme that Fourier transforms with spherical harmonics are easy to implement.

Second, one can replicate the tree structure of pixel numbering used e.g. with the Quadrilateralized Spherical Cube. This can easily be implemented since, due to the simple description of pixel boundaries, the analytical mapping of the HEALPix base-resolution elements (curvilinear quadrilaterals) into a  $[0,1] \times [0,1]$  square exists. This tree structure, a.k.a. nested scheme, allows one to implement efficiently all applications involving nearest-neighbour searches (see Wandelt, Hivon, and Górski 1998), and also allows for an immediate construction of the fast Haar wavelet transform on HEALPix .

The base-resolution pixel index number  $f$  runs in  $\{0, N_\theta N_\phi - 1\} = \{0, 11\}$ . Introducing the row index

$$f_{\text{row}} = \text{I}(f/N_\phi) \tag{10}$$

we define two functions which index the location of the southernmost corner (or vertex) of each base resolution pixel on the sphere, in latitude and longitude respectively:

$$F_1(f) = f_{\text{row}} + 2, \tag{11}$$

$$F_2(f) = 2(f \bmod N_\phi) - (f_{\text{row}} \bmod 2) + 1. \tag{12}$$

Consider the nested index  $p_n \in [0, 12N_{\text{side}}^2 - 1]$ , and define  $p'_n = (p_n \bmod N_{\text{side}}^2)$ , where  $p'_n$  denotes the nested pixel index within each base-resolution element., which has the following binary representation  $p'_n = [\dots b_2 b_1 b_0]_2$  (and  $b_i = 0$ , or  $1$ , and has the weight  $2^i$ ).

Given a grid resolution parameter  $N_{\text{side}}$  the location of a pixel center on each base-resolution pixel is represented by the 2 indices  $x$  and  $y \in \{0, N_{\text{side}} - 1\}$ . They both have their origin in the southernmost corner of each base-resolution pixel, with the  $x$  index running along the North-East direction, while the  $y$  index runs along the North-West direction. The binary representation of  $p'_n$  determines the values of  $x$ , and  $y$  as the following combinations of even and odd bits, respectively

$$x = [\dots b_2 b_0]_2 \tag{13}$$

$$y = [\dots b_3 b_1]_2 \tag{14}$$

Next, we introduce the vertical and horizontal coordinates (within the base-resolution pixel)

$$v = x + y \quad (15)$$

$$h = x - y \quad (16)$$

and obtain the following relations for the ring index  $i \in \{1, (N_\theta + 1)N_{\text{side}} - 1\}$

$$i = F_1(f)N_{\text{side}} - v - 1, \quad (17)$$

and the longitude index

$$j = \frac{F_2(f)N_{\text{side}} + h + s}{2}, \quad (18)$$

which can be translated into  $(z, \phi)$  coordinates using Eqs. 4, 5, 8, and 9.

### 5.3. Pixel Boundaries

Pixel boundaries are non-geodesic and take a very simple form:  $\cos \theta = a + b \times \phi$  in the equatorial zone, and  $\cos \theta = a + b/\phi^2$  in the polar caps. This allows one to explicitly check by simple analytical integration the exact area equality among pixels, and to compute efficiently more complex objects, e.g. the Fourier transforms of individual pixels.

Since the pixel center location is parametrized by integer value of  $j$ , setting  $j = k + 1/2$  or  $j = k + 1/2 + i$  with  $k$  a positive integer in Eq. (5) and substituting into Eq. (4) will give for the pixels boundaries of the North polar cap ( $z > 2/3$ )

$$z = 1 - \frac{k^2}{3N_{\text{side}}^2} \left( \frac{\pi}{2\phi_t} \right)^2, \quad (19)$$

$$z = 1 - \frac{k^2}{3N_{\text{side}}^2} \left( \frac{\pi}{2\phi_t - \pi} \right)^2, \quad (20)$$

where  $\phi_t = \phi \bmod \pi/2$ . The base pixels have boundaries defined as

$$z > \frac{2}{3}, \quad \phi = k' \frac{\pi}{2}, \quad (21)$$

with  $k' = 0, 1, 2, 3$

Similarly, for  $2/3 \leq z \leq -2/3$  the pixel boundaries can be found by setting  $j = k + s/2 \pm (i - N_{\text{side}})/2$  in Eq. (9) and substituting into Eq. (8)

$$z = \frac{2}{3} - \frac{4k}{3N_{\text{side}}} \pm \frac{8\phi}{3\pi} \quad (22)$$

Using these pixel boundaries, one can easily check by integration that each individual pixel has the same surface area  $\Omega_{\text{pix}}$ .

Table 1 summaries the number of pixels and resolution available in HEALPix . Since all pixels have the same surface area but slightly different shape, the angular resolution is defined as

$$\theta_{\text{pix}} \equiv \sqrt{\Omega_{\text{pix}}} \tag{23}$$

$$= \sqrt{\frac{3}{\pi} \frac{3600}{1'} \frac{1}{N_{\text{side}}}} \tag{24}$$

## 6. Spherical Harmonic Transforms

The requirement of iso-latitudinal location of pixel centers was built into HEALPix in order for the grid to support the fast discrete spherical harmonic transforms. The reason for the fast ( $\tilde{N}_{pix}^{3/2}$ ) scaling of the harmonic transform computational time with the size of the grid (or the grid resolution) is entirely geometrical - the associated Legendre function components of spherical harmonics, which can only be generated via slow recursions, have to be evaluated only once for each pixel ring. For other grids, which are not iso-latitude constrained, the extra computing time wasted on non-optimal generation of the associated Legendre functions, typically results with computational performance of order  $\sim N_{pix}^2$ . This geometrical aspect of discrete spherical transform computation is illustrated in Fig.6, which compares HEALPix with other tessellations including Quadrilateralized Spherical Cube (or QuadCube, used by NASA as data structure for COBE mission products), icosahedral tessellation of the sphere, and Equidistant Coordinate Partition, or the "geographic grid." This plot makes it visually clear why the iso-latitude ECP and HEALPix points-sets support faster computation of spherical harmonic transforms than the QuadCube, the icosahedral grid, and any non iso-latitude construction.

Figure (7) demonstrates the fundamental difference between computing speeds, which can be achieved on iso-latitude and non iso-latitude point-sets. In order to be able to perform the necessary computational work in support of the multi-million pixel spherical data sets one has to resort to iso-latitude structures of point-sets/sky maps, e.g. HEALPix. Moreover, the future needs are already fairly clear – measurements of the CMB polarization will require massively multi-element arrays of detectors, and will produce data sets characterized by a great multiplicity (of order of a few thousand) of sky maps. Since there are no computationally faster methods than those already employed in HEALPix, and global synthesis/analysis of a multimillion pixel map consumes about 103s of a standard serial machine CPU time, the necessary speed-up will have to be achieved via optimized parallelization of the required

computing.

A detailed description of implementation of the spherical harmonic transforms in the HEALPix software package, and the analysis of performance and accuracy thereof will given in a dedicated publication.

## 7. Summary

The Hierarchical Equal Area iso-Latitude Pixelization, HEALPix, is a methodology of discretization and fast numerical analysis and synthesis of functions or data distributed on the sphere. HEALPix is an intermediate data-structural, algorithmic, and functional layer between astronomical data, and the domain of application of variety of science extraction tools. HEALPix as a sky map format and associated set of analysis and visualization tools is already extensively adopted as an interface between Information Technology and Space (and suborbital) Science. This is manifested by applications of HEALPix by the following projects: CMB experiments Boomerang (deBernardis et al, 2000, Ruhl et al 2003), Archeops (Benoit et al, 2003ab), and TopHat, satellite mission WMAP (WMAP2003), the forthcoming satellite mission Planck, the Sloan Digital Sky Survey, and others.

Our involvement with development, distribution, and support of HEALPix since 1997 would have been impossible without support of a number of institutions and individuals. We are indebted to Theoretical Astrophysics Center in Copenhagen, Igor Novikov, and Per Rex Christensen; to European Southern Observatory, Peter Quinn, and Kevin Maguire; to MPA, Garching, and Simon D.M. White; to Caltech's Observational Cosmology Group, and Andrew Lange; to Caltech/IPAC, George Helou, and Ken Ganga; to JPL/Caltech, Center for Long Wavelength Astrophysics, and Charles R. Lawrence. We are also grateful for all the positive feedback received from numerous HEALPix users worldwide.

## REFERENCES

- Baumgardner, J. R. & Frederickson, P. O. 1985, SIAM J. Numerical Analysis, 22, 1107
- Benoit, A., et al, A&A 2003, 399, L23-L30
- Benoit, A., et al, A&A, 2003, 399, L19-L23
- Crittenden, R. & Turok, N. G. 1998, astro-ph/9806374

- de Bernardis, P. et al., 2000, *Nature* 404, 955
- Doroshkevich, A.G. et al., 2003, astro-ph/0305537
- Driscoll, J. R. & Healy, D. 1994, *Adv. in Appl. Math.*, 15, 202
- Górski, K. M., Hivon, E., & Wandelt, B. D. 1998, in the Proceedings of the MPA/ESO Conference "Evolution of Large-Scale Structure: from Recombination to Garching", eds. A.J. Banday, R.K. Sheth & L. Da Costa, Printpartners Ipskamp NL, pp. 37-42 (astro-ph/9812350)
- Muciaccia, P. F, Natoli, P. & Vittorio, N. 1998, *Ap.J.*, 488, L63
- Ruhl, J. E., et al, 2003, *ApJ* 599, 786
- Saff, E. B. & Kuijlaars, A. B. J. 1997, *The Mathematical Intelligencer*, 19, #1, 5
- Szalay, A.S. & Brunner R.J. 1999, *Future Generation Computer Systems*, 16, 63; astro-ph/9812335
- Tegmark, M. 1996, *ApJ*, 470, L81
- Wandelt, B.D., Hivon, E. & Górski, K.M. 1998, in "Fundamental Parameters in Cosmology", proceedings of the XXXIIIrd Rencontres de Moriond, eds. Tran Thanh Van; astro-ph/9803317
- White, R.A., and Stemwedel, S.W. 1992, in ASP Conf. Ser. 25, *Astronomical Data Analysis, Software and Systems I*, eds. D.M. Worrall, C. Biemesderfer, & J. Barnes (San Francisco:ASP), 379
- Wilkinson Microwave Anisotropy Probe, First-Year results from WMAP, 2003, *ApJS*, 148,1-241, see also <http://lambda.gsfc.nasa.gov>

$k$	$N_{\text{side}} = 2^k$	$N_{\text{pix}} = 12N_{\text{side}}^2$	$\theta_{\text{pix}} = \Omega_{\text{pix}}^{1/2}$
0	1	12	$58.6^\circ$
1	2	48	$29.3^\circ$
2	4	192	$14.7^\circ$
3	8	768	$7.33^\circ$
4	16	3072	$3.66^\circ$
5	32	12288	$1.83^\circ$
6	64	49152	$55.0'$
7	128	196608	$27.5'$
8	256	786432	$13.7'$
9	512	3145728	$6.87'$
10	1024	12582912	$3.44'$
11	2048	50331648	$1.72'$
12	4096	201326592	$51.5''$
13	8192	805306368	$25.8''$
14	$2^{14}$	$3.22 \times 10^9$	$12.9''$
15	$2^{15}$	$1.29 \times 10^{10}$	$6.44''$
16	$2^{16}$	$5.15 \times 10^{10}$	$3.22''$
17	$2^{17}$	$2.06 \times 10^{11}$	$1.61''$
$\vdots$	$\vdots$	$\vdots$	$\vdots$
29	$2^{29}$	$3.46 \times 10^{18}$	$3.93 \times 10^{-4}''$

Table 1: Table of the number of pixels and pixel size accessible to HEALPix . The use of 32-bit signed integers for the pixel indexing currently restrict the resolution accessible to  $N_{\text{side}} \leq 8192$ . The use of 64-bit signed integers will allow to reach  $N_{\text{side}} = 2^{29}$ .

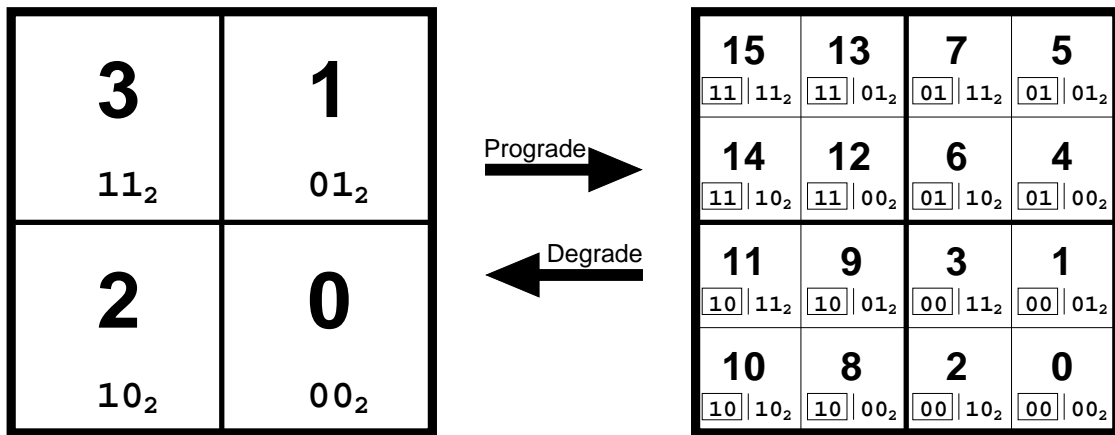


Fig. 1.— Quadrilateral tree pixel numbering. The coarsely pixelised coordinate patch on the left consists of four pixels. Two bits suffice to label the pixels. To increase the resolution, every pixel splits into 4 daughter pixels shown on the right. These daughters inherit the pixel index of their parent (boxed) and acquire two new bits to give the new pixel index. Several such curvilinearly mapped coordinate patches (12 in the case of HEALPix, and 6 in the case of the *COBE* quad-sphere) are joined at the boundaries to cover the sphere. All pixels indices carry a prefix (here omitted for clarity) which identifies which base-resolution pixel they belong to.

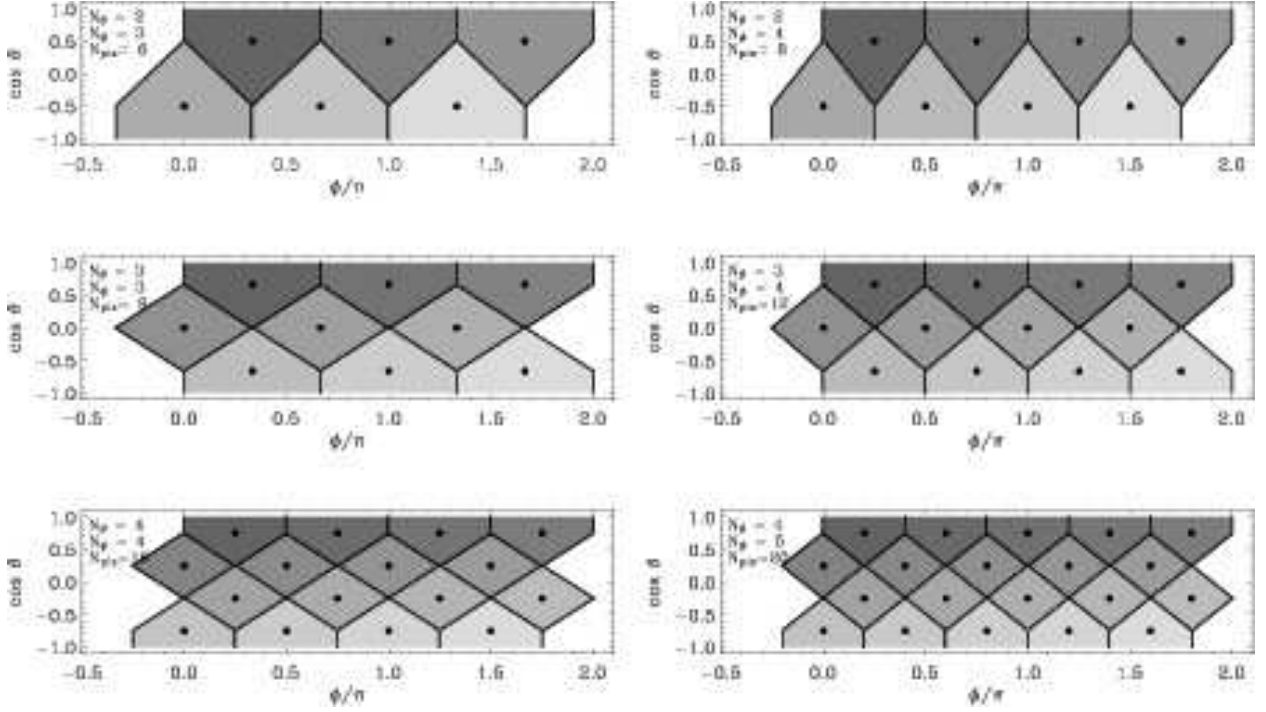


Fig. 2.— cylindrical projection of a number of equal area, iso-latitude tessellations of the sphere, which can support a hierarchical tree of further subdivisions of each large base-resolution pixel. Six out of possible realizations of such tessellation are shown for several values of grid parameters  $N_\theta$ , and  $N_\phi$ . The HEALPix grid, used for development of the corresponding software package, is described by  $N_\theta = 3$ , and  $N_\phi = 4$ .



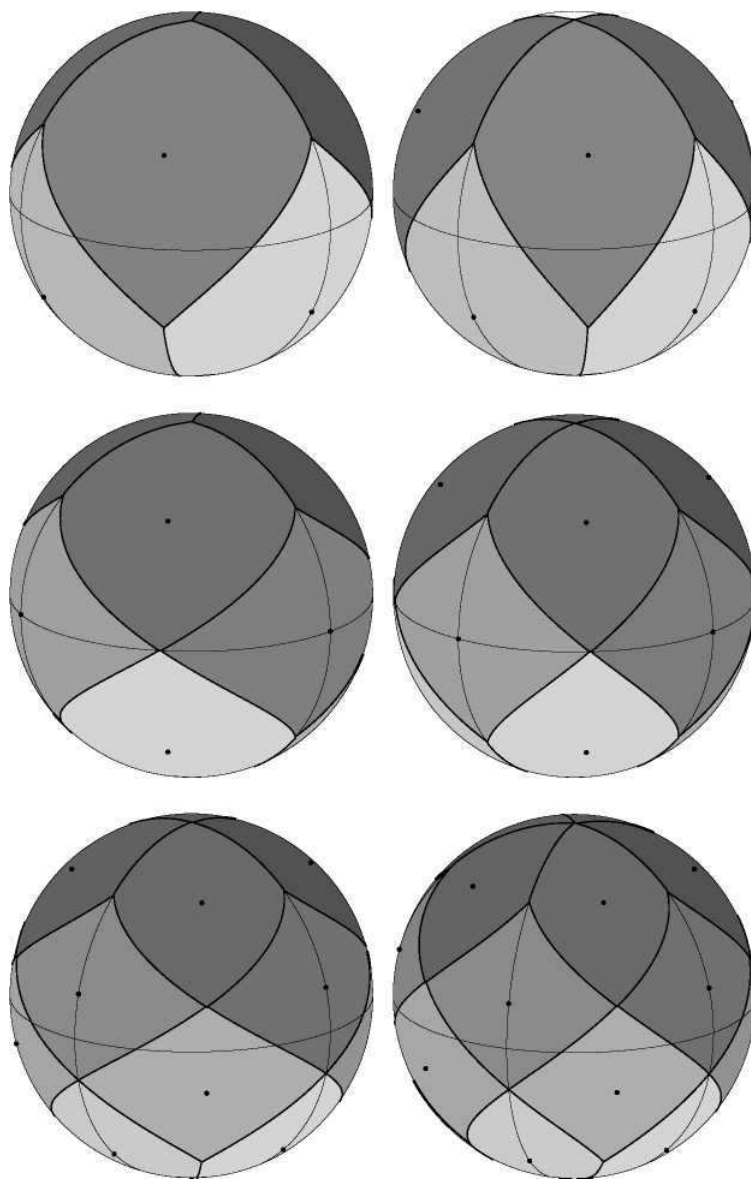


Fig. 3.— Orthographic projection of the same base-resolution spherical tessellations as those shown in Fig.2.

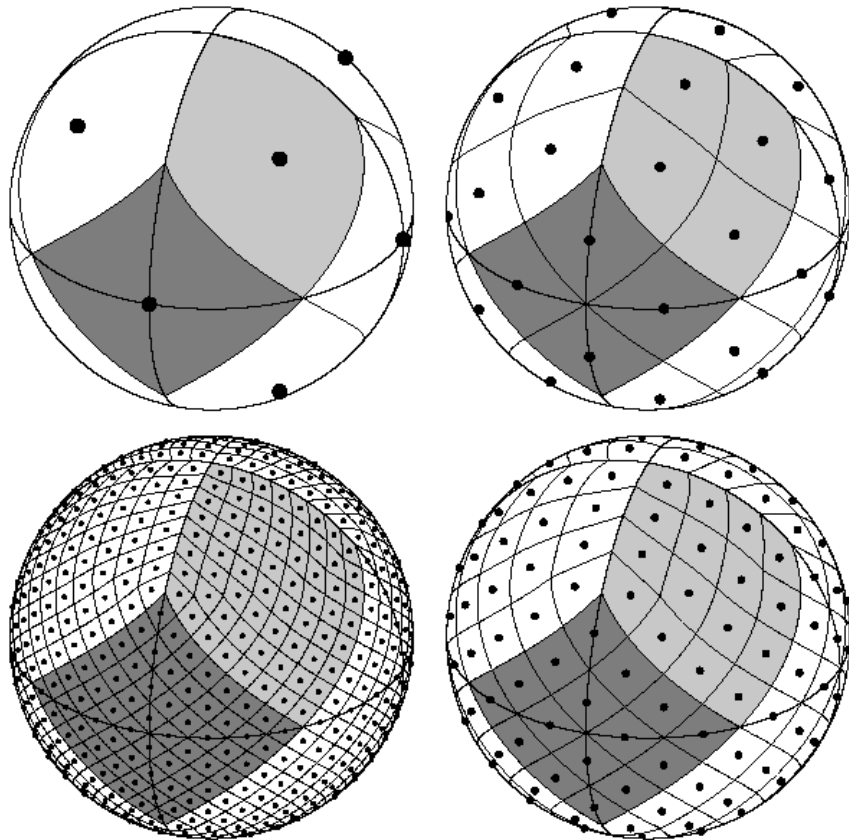


Fig. 4.— Orthographic view of the HEALPix partition of the sphere. Overplot of equator and meridians illustrates the octahedral symmetry of HEALPix. Light-gray shading shows one of the eight (four north, and four south) identical polar base-resolution pixels. Dark-gray shading shows one of the four identical equatorial base-resolution pixels. Moving clockwise from the upper left panel the grid is hierarchically subdivided with the grid resolution parameter equal to  $N_{side} = 1, 2, 4, 8$ , and the total number of pixels equal to  $N_{pix} = 12 \times N_{side}^2 = 12, 48, 192, 768$ . All pixel centers are located on  $N_{ring} = 4 \times N_{side} - 1$  rings of constant latitude. Within each panel the areas of all pixels are identical.

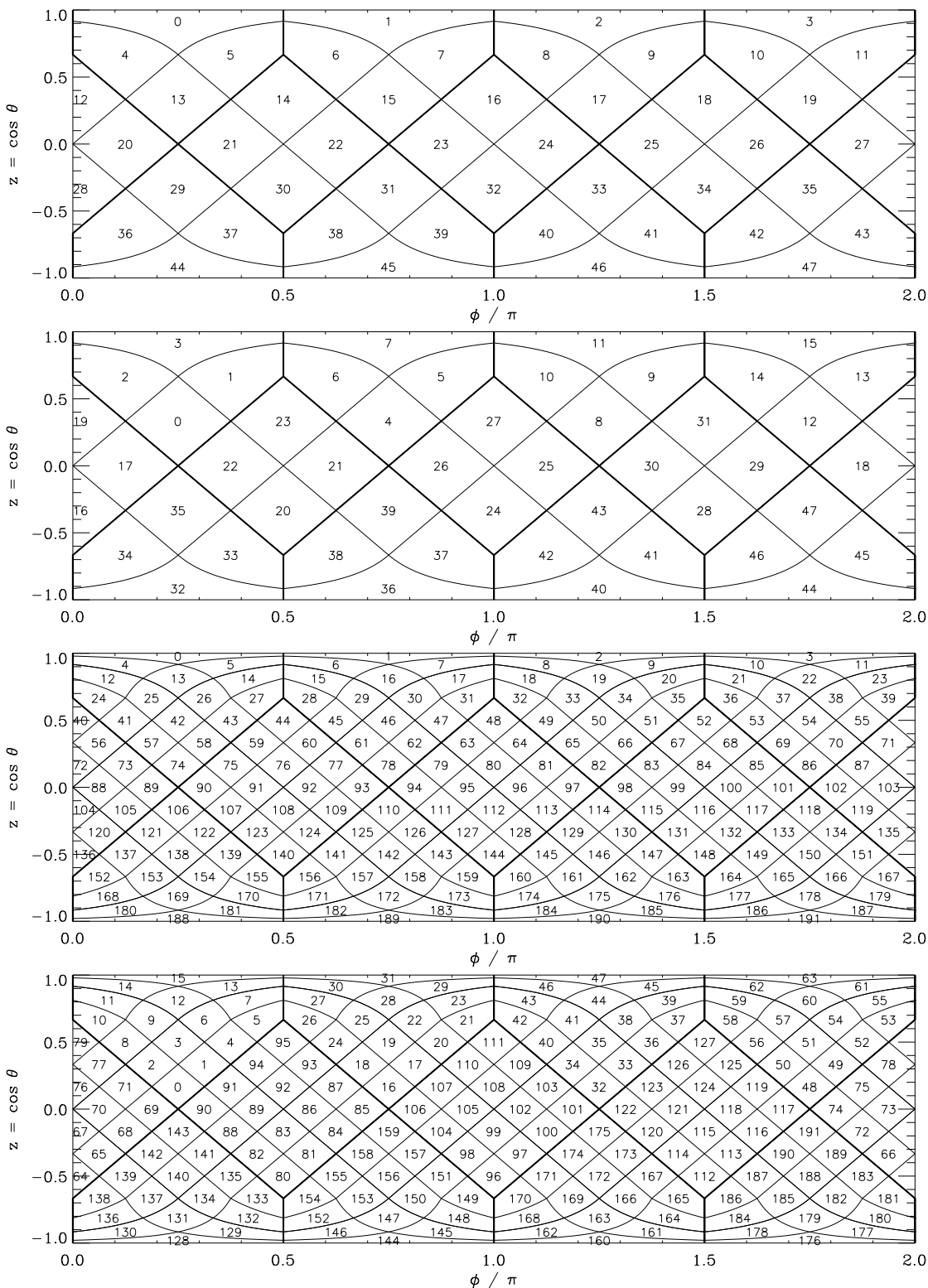


Fig. 5.— The layout of the HEALPix pixels on the sphere, and demonstration of two possible pixel indexations — one running on iso-latitude rings, and the other arranged hierarchically, or in a nested tree fashion. The latter capability is essential for the possible database applications of HEALPix.

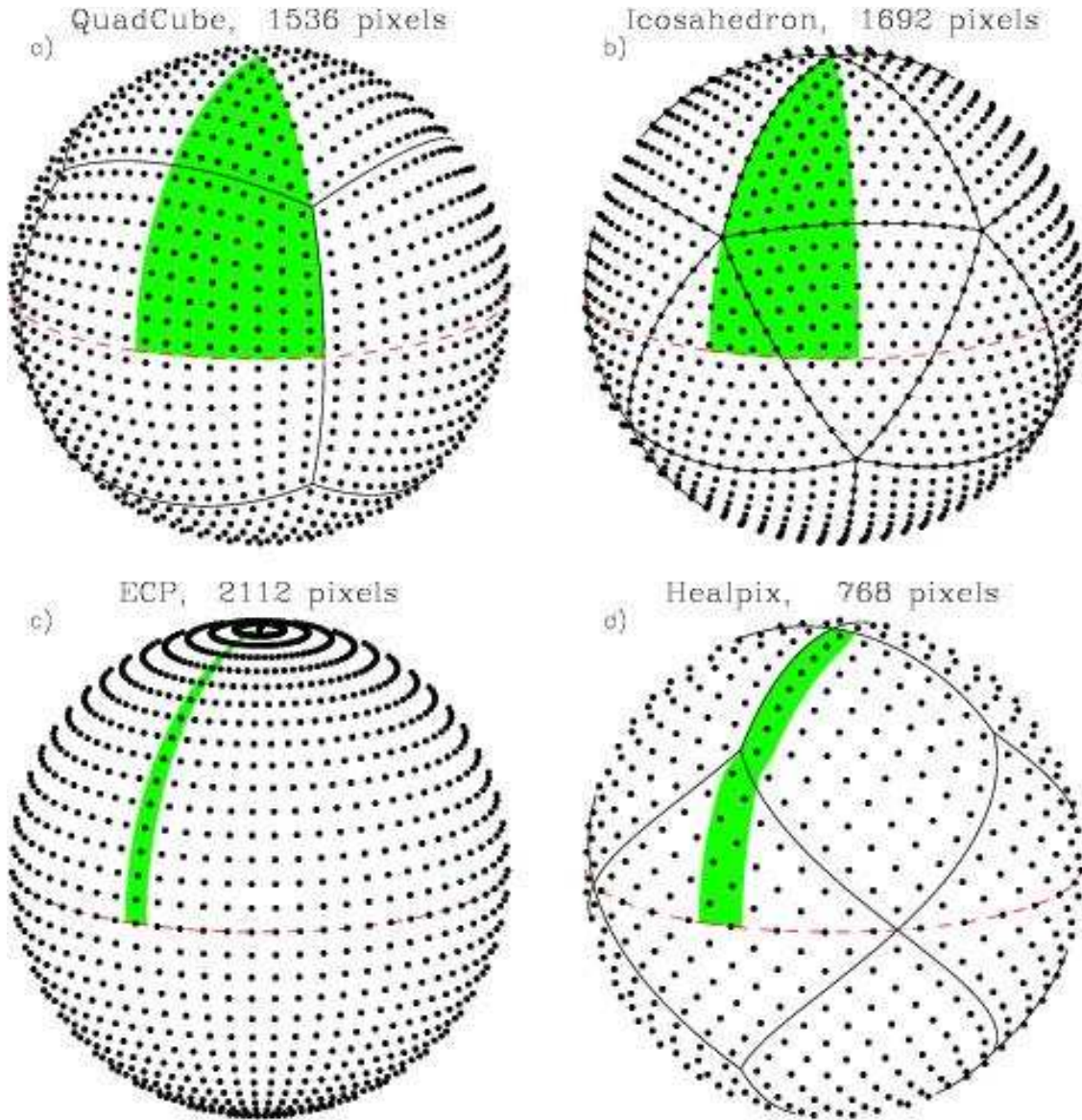


Fig. 6.— Comparison of HEALPix with other tessellations including Quadrilateralized Spherical Cube (or QuadCube, used by NASA as data structure for COBE mission products), icosahedral tessellation of the sphere, and Equidistant Coordinate Partition, or the ‘geographic grid.’ The shaded areas illustrate the subsets of all pixels on the sky for which the associated Legendre functions have to be computed in order to perform the spherical harmonic transforms. This plot demonstrates why the iso-latitude ECP and HEALPix points-sets support faster computation of spherical harmonic transforms than the QuadCube, the icosahedral grid, and any non iso-latitude construction.

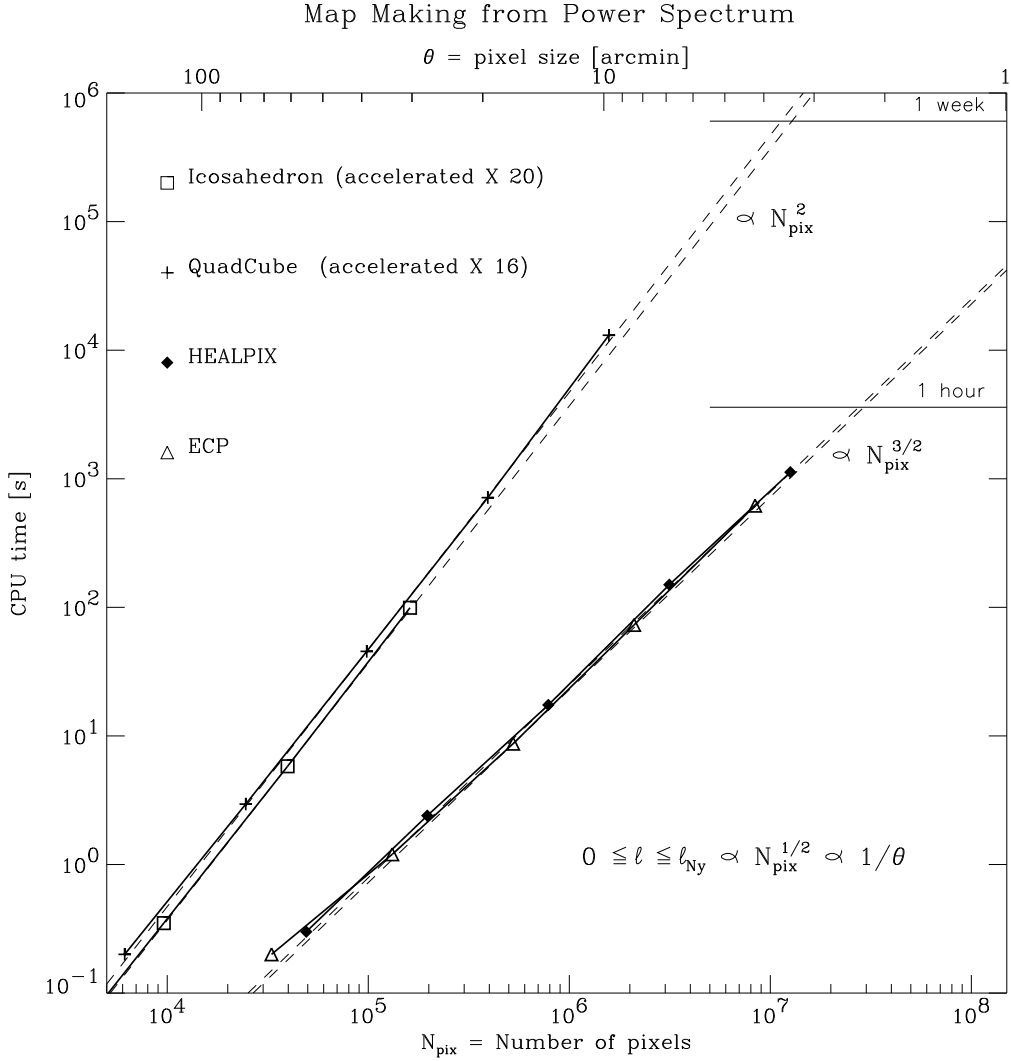


Fig. 7.— Illustration of the fundamental difference between computing speeds, which can be achieved on iso-latitude and non iso-latitude point-sets. In order to be able to perform the necessary computational work in support of the multi-million pixel spherical data sets one has to resort to iso-latitude structures of point-sets/sky maps, e.g. HEALPix Moreover, the future needs are already fairly clear measurements of the CMB polarization will require massively multi-element arrays of detectors, and will produce data sets characterized by a great multiplicity (of order of a few thousand) of sky maps. Since there are no computationally faster methods than those already employed in HEALPix, and global synthesis/analysis of a multimillion pixel map consumes about  $10^3$ s of a standard serial machine CPU time, the necessary speed-up will have to be achieved via optimized parallelization of the required computing.